Journal of Magnetic Resonance **147,** 261–265 (2000)
doi:10.1006/jmre.2000.2210, available online at http://www.idealibrary.com on IDEAL®

Continuous-Flow Optical Pumping NMR in a Closed Circuit System

J. M. Kneller,* R. J. Soto,* S. E. Surber,* J.-F. Colomer,† A. Fonseca,† J. B.Nagy,† and T. Pietraß*

**Department of Chemistry, New Mexico Tech, Socorro, New Mexico 87801; and †Laboratoire de Résonance Magnétique Nucléaire, Facultés Universitaires Notre-Dame de la Paix, 61 rue Bruxelles, 5000 Namur, Belgium*

Received April 27, 2000; revised August 30, 2000

In a typical continuous-flow optical pumping setup, the chemical shift of xenon in the adsorbed phase depends on the gas flow rate due to warming of the sample surface by the gas stream. Calibration of the system using the ^{207}Pb resonance of solid lead nitrate is necessary to determine the actual sample temperature. Optimum pulse repetition rates are strongly affected by gas flow and spin–lattice relaxation rates. The interplay of flow and pulse repetition rate alters signal intensity ratios and may lead to the complete suppression of signals. © 2000 Academic Press

Key Words: **optical pumping; continuous gas flow; pulse repetition rates.**

INTRODUCTION

NMR of ^{129}Xe has proven to be an effective tool for the characterization of microporous materials (*1–4*). However, limitations in signal intensity arise due to the low spin density of a gas under thermal equilibrium conditions. In recent years, techniques for the enhancement of the NMR signal using laser-polarized gases such as ^{3}He and ^{129}Xe have been developed (*5, 6*). With high-power laser diode arrays, a continuous flow of optically polarized xenon can be generated and passed over the sample surface (*7*). This technique is an improvement over the batch-mode production of laser-polarized xenon because it allows for the use of multiple-pulse NMR experiments, the incorporation of magic angle spinning (*8, 9*), and signal averaging for samples with short ^{129}Xe spin–lattice relaxation times or poor xenon adsorption properties (*10*). Whereas most groups work with an open circuit system where the gas mixture is discarded upon exit of the sample region, our setup is a closed circuit system where the xenon polarization is continuously being replenished by redirecting the gas mixture back into the optical pumping cell upon exit of the sample region. While the open circuit system offers the advantage of permanently supplying fresh, pure gas to the optical pumping cell, contamination of the gas mixture through the sample and tubing connections is a risk in the closed circuit system. The advantages, however, lie in lower operating costs and greater variability in the total gas pressure.

In this contribution, we demonstrate the effect of gas circulation on ^{129}Xe NMR chemical shifts and signal intensities. These effects were studied using a sample of multiwalled carbon nanotubes. The material was synthesized by catalytic decomposition of acetylene over a cobalt/zeolite catalyst. The catalyst was removed by acidic dissolution in concentrated HF. Oxidation of these prepurified nanotubes with aqueous permanganate solution leads to removal of amorphous carbon as well as the fullerene endcaps, so that open tubes with an average inner and outer diameter of 6 and 16 nm, respectively, result. The average nanotube has 15 concentric walls and is 50 μm long. Synthesis and characterization have been described in detail elsewhere (*11*). A detailed discussion of the penetration of xenon into the nanotubes as derived from ^{129}Xe NMR spectroscopy can be found in Ref. (*12*). In this contribution, only the interplay between continuous gas flow and NMR acquisition parameters will be discussed.

RESULTS

Spectra recorded at 165 K and at different pumping speeds are shown in Fig. 1 (top). The two vertical lines in Fig. 1 (top) mark the ^{129}Xe NMR chemical shifts for xenon in the adsorbed phase when circulating the xenon gas mixture at pumping speeds j_1 and j_3 (see Table 1). The difference, Δ, is plotted as a function of temperature (Fig. 1, bottom). Under equilibrium or static conditions, i.e., without optical pumping and without gas flow, the observed chemical shift of xenon in the adsorbed phase is consistently slightly lower when compared to the shift observed at flow rate j_1. While Δ is small at ambient temperature, it increases as the temperature is being lowered. In fact, Δ is linearly dependent on temperature over the range investigated. This effect is due to an increased temperature caused by the stream of warm gas passed over the sample surface. Actual sample temperatures were determined using the ^{207}Pb NMR resonance of solid $Pb(NO_3)_2$ for calibration (*13*). The dependence of the ^{207}Pb NMR isotropic shifts on flow rate and temperature is presented in Fig. 2. The resulting corrected ^{129}Xe NMR shifts for xenon in the adsorbed phase are displayed in Fig. 3 (unfilled symbols) in comparison to the uncorrected shifts (filled symbols).

The xenon dwell time in the NMR coil region was determined with a calibrated flow meter at ambient pressure and

1090-7807/00 $35.00

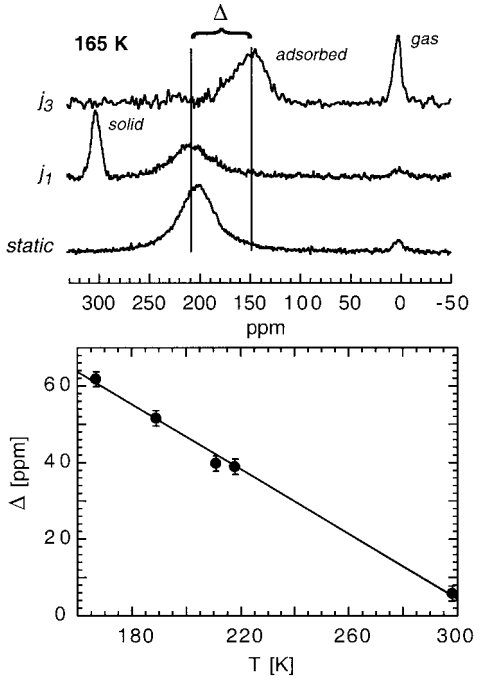

FIG. 1. Top: Flow-rate (see Table 1) dependent ^{129}Xe NMR spectra of xenon in contact with multiwalled carbon nanotubes at 165 K (as indicated by the thermocouple). Peaks are labeled according to their phases (gas, adsorbed, solid). Vertical lines illustrate the chemical shift difference Δ for xenon in the adsorbed phase observed for flow rates j_1 and j_3. Bottom: Δ is plotted as a function of temperature.

with an inversion recovery technique (*14*) applied to the gas resonance which gave rise to a strong signal. No dependence on temperature was observed for the faster flow rate j_3, while the xenon dwell time in the coil region changed with flow rate as expected.

Characteristic pulse repetition rates ρ were determined by varying the pulse delay Δt between transients and fitting the resulting integrated signal intensities to a function of the form $(1 - e^{-\Delta t/\tau})$ where $\tau = \rho^{-1}$ in analogy to a saturation recovery experiment. In our experiment, however, the increase in signal intensity for growing pulse delays is governed by the replacement of depolarized xenon in the sample region with freshly polarized xenon. ρ depends strongly on temperature and flow rate for the peak corresponding to xenon in the gas phase,

TABLE 1

Method	Flow meter	Inversion recovery
Flow rate j_1 (ml/s)	0.58 ± 0.06	0.58 ± 0.06
Flow rate j_2 (ml/s)	7 ± 3	—
Flow rate j_3 (ml/s)	14 ± 10	2.6 ± 0.3
Flow rate j_4 (ml/s)	21 ± 10	—
Dwell time at j_1 (s)	0.87 ± 0.09	0.87 ± 0.09
Dwell time at j_3 (s)	0.03 ± 0.02	0.19 ± 0.03

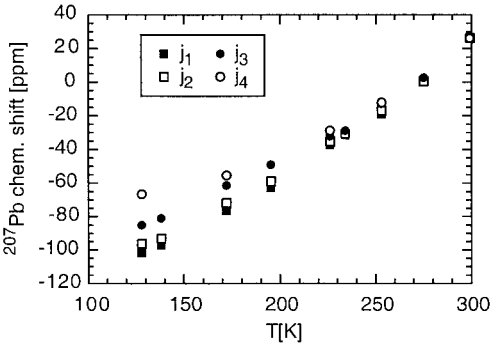

FIG. 2. ^{207}Pb NMR isotropic shifts of lead nitrate for different flow rates (see Table 1) and temperatures. The temperatures refer to those measured by the thermocouple which was located in the dewared sample region, but outside the sample container.

while within experimental error no such dependence is observed for xenon in the adsorbed phase at temperatures below 250 K (Fig. 4). Above 250 K, there is some indication of an increase in ρ^{-1} for xenon in the adsorbed phase but the errors are fairly large in this temperature range due to the diminished signal intensity (compare Fig. 1b in Ref. (*12*)). For all flow rates and temperatures, the ratio of the integrated signal intensities of xenon in the adsorbed phase over xenon in the gas phase is largest for high pulse repetition rates. This is equivalent to the observation that the NMR signal buildup was faster for xenon in the adsorbed phase. For both flow rates, this ratio is slightly increasing with decreasing temperature.

DISCUSSION

The average dwell time of xenon in the coil region is an important parameter for the interpretation of magnetization buildup. The results from the inversion recovery technique and the flow meter agree very well for j_1 (Table 1). Therefore, the inversion-recovery method yields probably the most reliable

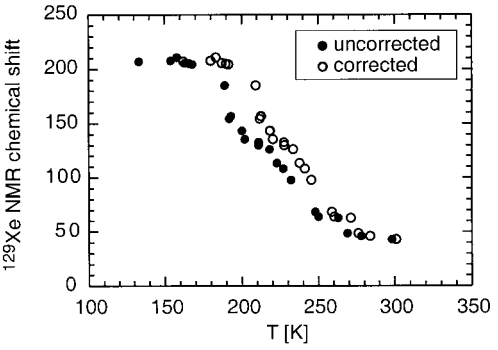

FIG. 3. Temperature-dependent ^{129}Xe NMR chemical shifts for xenon physisorbed on multiwalled carbon nanotubes obtained at flow rate j_3. Error bars (±3 ppm) are equal to or smaller in size than the symbols. Unfilled circles correspond to chemical shifts corrected for temperature using the calibration shown in Fig. 2 and filled circles to the uncorrected data.

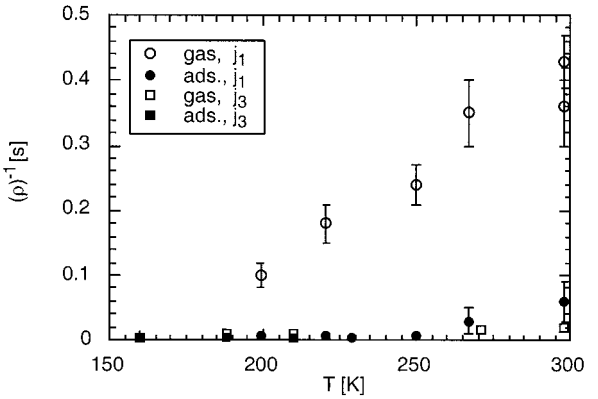

FIG. 4. Temperature and flow-rate dependence of ρ^{-1}, the reciprocal characteristic pulse repetition rate, obtained by monitoring the xenon signal intensity as a function of pulse delay. The rates are shown both for gaseous and for adsorbed ^{129}Xe in contact with multiwalled carbon nanotubes. The data for j_3 are displayed without the temperature correction shown in Fig. 1. To reflect the true sample temperatures, each data point would be shifted to a higher temperature.

value for j_3. The large errors for j_2–j_4 determined using the flow meter are due to the fact that the flow rate could not be measured directly, but had to be extrapolated and is thus considered unreliable.

Flow rates j_1 and j_3 resulted in a different chemical shift for the peak corresponding to xenon in the adsorbed phase (Fig. 1, top). This difference is the more pronounced the lower the temperature (Fig. 1, bottom). Higher flow rates yielded lower chemical shift values. This trend is expected if, due to the increased flow rate, the sample temperature is higher than indicated by the thermocouple which is located in the dewared probe region, but not in direct contact with the sample. Hence, an increased sample temperature must contribute to the lower shifts observed at flow rate j_3. The higher sample temperature at flow rate j_3 explains the presence of the strong gas peak (Fig. 1). Xenon in the solid phase can be observed only at flow rate j_1 and not under static conditions (Fig. 1, top). The enhanced xenon polarization under optical pumping conditions allows us to detect this resonance despite its long relaxation time. Moreover, this signal may be due to xenon frozen onto the container wall outside the coil region and would thus not be detectable under equilibrium conditions. The warming of the sample surface due to the gas flow becomes more pronounced at lower temperatures where the temperature difference between the xenon gas mixture and the cooling gas is increasing (Fig. 1, bottom). However, the largest chemical shift is expected for acquisition under static, equilibrium conditions, which is not observed (Fig. 1, top). It is not completely understood why the chemical shifts observed at j_1 are, at all temperatures studied, consistently slightly higher than under equilibrium conditions. A possible contribution may arise from magnetic field inhomogeneity, as under slow flow conditions most of the adsorbed phase NMR signal is due to xenon in the entrance region of the coil. At higher flow rates, the xenon can penetrate further into the coil region before relaxing, and under static conditions the signal originates from the entire coil region.

Temperature-dependent chemical shifts were therefore calibrated using the isotropic ^{207}Pb NMR shift σ of solid lead nitrate. Under the static conditions applied, the ^{207}Pb NMR signal displays the lineshape typical for a chemical shift anisotropy with axially symmetric tensor. The temperature-dependent isotropic chemical shifts obtained under MAS conditions and careful temperature calibration are tabulated (*13*). While the slope $d\sigma/dT$ for j_1 agrees well with data reported in Ref. (*13*), the deviation becomes stronger for faster pumping speeds (Fig. 2). Moreover, the nonlinearity at lower temperatures becomes more pronounced as the difference in temperature between the cooling gas and the xenon gas mixture increases. ^{129}Xe chemical shift data for xenon physisorbed on multiwalled carbon nanotubes are presented in Fig. 3 with and without the temperature correction from Fig. 2. The large discrepancy in chemical shifts obviates the need for temperature calibration in order to obtain reliable chemical shift data. It should be noted that carbon nanotubes are better thermal conductors than lead nitrate. Therefore, it is possible that if a temperature equilibrium between the cooling gas and the warm xenon gas mixture has not been established, the actual sample temperature is still different for the nanotubes and lead nitrate under otherwise identical experimental conditions. We attempted to counter this possibility by allowing for long temperature equilibration times. Moreover, our method does not allow us to compensate for possible temperature gradients in the sample. Such a temperature gradient could arise if the heat transfer between the sample and the warm gas mixture is so rapid that much of the heat has been exchanged in the entrance region of the coil resulting in a lower temperature at the exit region. Such a temperature gradient would lead to line broadening of the ^{129}Xe resonance and could be tested for using a hole-burning technique. Since we observed the largest linewidths under static (no gas flow) conditions, we believe that such a temperature gradient can be disregarded for the carbon nanotubes.

The effect of pulse repetition rate on the magnitude of the observed signal is summarized in Fig. 4 for xenon in the gas and adsorbed phase. While no dependence on temperature or flow rate is observable for xenon in the adsorbed phase—the characteristic pulse repetition rate ρ is about $(5\ \text{ms})^{-1}$—a pronounced effect of these parameters is evident for xenon in the gas phase. At the smaller flow rate j_1, ρ^{-1} decreases from about 400 ms at ambient temperature to 100 ms at 199 K. For the higher flow rate j_3, ρ^{-1} is independent of temperature with $\rho^{-1} \approx 20$ ms. At first, it seems counterintuitive for ρ^{-1} to be a function of temperature and not of flow rate alone. ρ^{-1} decreases at lower temperatures due to the fact that the spin–lattice relaxation time for xenon in the gas phase increases as the temperature is lowered (from 0.018 ± 0.002 s at 298 K to 0.13 ± 0.04 s at 166 K) and becomes comparable to the xenon's dwell time in the coil region. As a result, xenon can

traverse the entire coil region with only minor relaxation and the characteristic pulse delay ρ^{-1} is of the order of T_1. At ambient temperature, T_1 for Xe in the gas phase is shorter, and the signal intensity is best for a more complete exchange of xenon in the coil region with freshly polarized xenon, corresponding to an increase in ρ^{-1}. The opposite is true for xenon in the adsorbed phase. In this case, the relaxation time decreases when lowering the temperature (from 0.010 ± 0.001 s at 298 K to 0.0035 ± 0.0004 s at 166 K) and is always short when compared to the reciprocal of the flow rate. Thus, it is necessary to excite the xenon immediately upon entry in the coil region before relaxation takes place.

For two-dimensional exchange experiments, a much longer recycle delay was required to ensure optimum signal intensity. Two to three dwell times were necessary to completely exchange the xenon in the sample region. For these experiments, it is mandatory that the entire coil region be filled with freshly polarized xenon, since the mixing time is on the same order of magnitude as the spin–lattice relaxation time. For single-pulse acquisition experiments, we expected that ρ^{-1} should exactly reflect xenon's dwell time in the sample region, but we determined a shorter ρ^{-1} since most of the signal arises from a volume smaller than that enclosed by the coil. At the higher flow rate, ρ^{-1} becomes independent of temperature since the gas mixture is transported much faster through the coil region.

CONCLUSIONS

The sample temperature in a continuous flow optical pumping system is strongly affected by the flow rate of the gas mixture. A decrease in ^{129}Xe NMR chemical shift with increasing flow rate is caused by a temperature rise due to the warm gas stream. This effect is strongest for the lowest temperatures and the highest flow rates as calibration with the isotropic chemical shift of the ^{207}Pb resonance in solid lead nitrate revealed. While precooling of the xenon gas mixture to the sample temperature would avoid this warming effect, it is conceivable that it would also lead to a decrease in xenon partial pressure at the lowest temperatures. The inversion recovery method was found to be the most reliable to determine flow rates. Characteristic pulse repetition rates depend on the flow rate intertwined with T_1. Our results show that continuous-flow optical pumping ^{129}Xe NMR data must be treated cautiously as flow rate and pulse repetition rate can give rise to the complete suppression of peaks or to a signal intensity ratio far from equilibrium conditions. For two-dimensional exchange experiments, for example, complete gas exchange in the coil region between scans is necessary. Too fast a pulse repetition rate leads to complete annihilation of the NMR signal. This effect was particularly strong in our sample which exhibits a very short ^{129}Xe NMR T_1.

EXPERIMENTAL

The continuous-flow optical pumping apparatus, similar to the one used by Seydoux *et al.* (*7*), is set up in the fringe field of the superconducting NMR magnet (9.4 T). The gas mixture consisting of 2.24% nitrogen, 8.9% xenon, and 88.86% helium is circulated in a closed system over the sample surface and back into the optical pumping cell. A fiber-coupled laser diode array (OPTO-Power Corporation, Tucson, AZ) delivering 45 W at 795 nm and operating at a current of 28 A is used for the excitation of rubidium. Circular polarization of the pumping light was achieved with a polarizing beamsplitter and half-wave and quarter-wave plates (Newport Corporation, Irvine, CA). The NMR sample cell (10-mm outer diameter, 8-mm inner diameter) is connected to the optical pumping setup through the length of the homebuilt NMR probe with 1.65-mm-inner-diameter PFA (perfluoroalkoxy, Swagelok) tubing using compression fittings. A few drops of Rb metal are placed in the optical pumping cell which is heated by a stream of hot air to approximately 448 K.

In order to reduce gas contamination, a rubidium reservoir is heated together with the optical pumping cell. The recirculated xenon passes through this reservoir where all impurities (mainly oxygen and water) should react with the rubidium before entering the pumping cell. Nevertheless, impurities in the gas mixture inadvertently picked up by the gas when traversing the system and the sample were transported into the optical pumping cell which led to its deterioration over the course of several days. Deposits in the pumping cell made it then necessary to exchange the rubidium. An additional gas purification device such as a titanium getter (*8*) will probably extend the lifetime of the pumping cell.

As expected, the xenon polarization increased with increasing gas pressure. For safety reasons, data were usually recorded at a total pressure of 422 kPa, which corresponds to a partial pressure of xenon of 1.28 kPa. Under the closed circuit flow conditions, the xenon polarization as determined by NMR in an empty sample cell was about 1.5%.

ACKNOWLEDGMENTS

We acknowledge financial support through ACS-PRF Grant No. 30916-G and for an NMRPI grant through UCDRD. A. Fonseca acknowledges financial support through the Belgian Program on Inter University Poles of Attraction initiated by the Belgian State, Prime Minister's Office for Scientific, Technical, and Cultural Affairs (OSTC-PAI-IUAP No. 4/10 on Reduced Dimensionality Systems).

REFERENCES

1. P. J. Barrie and J. Klinowski, ^{129}Xe NMR as a probe for the study of microporous solids: A critical review, *Prog. NMR Spectrosc.* **24,** 91–108 (1992).
2. C. Dybowski, N. Bansal, and T. Duncan, NMR spectroscopy of xenon in confined spaces: Clathrates, intercalates and zeolites, *Ann. Rev. Phys. Chem.* **42,** 433–464 (1991).

3. D. Raftery and B. F. Chmelka, *in* "Solid State NMR I: Methods" (B. Blümich, Ed.), Vol. 30, pp. 111–158, Springer-Verlag, Heidelberg, 1994.

4. C. I. Ratcliffe, in "Annual Reports on NMR Spectroscopy" (G. A. Webb, Ed.), Vol. 36, pp. 123–221, Academic Press, San Diego, 1998.

5. W. Happer, E. Miron, S. Schaefer, D. Schreiber, W. A. v. Wijngaarden, and X. Zeng, Polarization of the nuclear spins of noble-gas atoms by spin exchange with optically pumped alkali-metal atoms, *Phys. Rev. A* **29,** 3092–3110 (1984).

6. D. Raftery, H. Long, T. Meersmann, P. J. Grandinetti, L. Reven, and A. Pines, High-field NMR of adsorbed xenon polarized by laser pumping, *Phys. Rev. Lett.* **66,** 584–587 (1991).

7. R. Seydoux, A. Pines, M. Haake, and J. A. Reimer, NMR with a continuously circulating flow of laser-polarized ^{129}xenon, *J. Phys. Chem. B* **103,** 4629–4637 (1999).

8. E. Brunner, R. Seydoux, M. Haake, A. Pines, and J. A. Reimer, Surface NMR using laser-polarized ^{129}Xe under magic angle spinning, *J. Magn. Reson.* **130,** 145–148 (1998).

9. D. Raftery, E. MacNamara, G. Fisher, C. V. Rice, and J. Smith, Optical pumping and magic angle spinning: Sensitivity and resolution enhancement for surface NMR obtained with laser-polarized xenon, *J. Am. Chem. Soc.* **119,** 8746–8747 (1997).

10. T. Pietraß, Optically Polarized ^{129}Xe in Magnetic Resonance Techniques, *Magn. Reson. Rev.* **17,** 263–337 (2000).

11. J. F. Colomer, P. Piedigrosso, I. Willems, C. Journet, P. Bernier, G. van Tendeloo, A. Fonseca, and J. B.Nagy, Purification of catalytically produced multi-wall nanotubes, *J. Chem. Soc., Faraday. Trans.* **94,** 3753–3758 (1998).

12. J. M. Kneller, R. J. Soto, S. E. Surber, T. Pietraß, J.-F. Colomer, A. Fonseca, J. B.Nagy, and G. van Tendeloo, TEM and laser-polarized ^{129}Xe NMR characterization of oxidatively purified carbon nanotubes, *J. Am. Chem. Soc.,* in press.

13. A. Bielecki and D. P. Burum, Temperature dependence of ^{207}Pb MAS spectra of solid lead nitrate. An accurate, sensitive thermometer for variable-temperature MAS, *J. Magn. Reson. A* **116,** 215–220 (1995).

14. M. Haake, A. Pines, J. A. Reimer, and R. Seydoux, Surface enhanced NMR using continuous-flow laser-polarized xenon, *J. Am. Chem. Soc.* **119,** 11711–11712 (1997).